

# CFD-based Modeling of Transport Phenomena for Engineering Problems

Maksim Mezhericher

**Abstract**—Computational Fluid Dynamics is a popular modeling approach which utilizes numerical methods and computer simulations to solve and analyze problems that involve transport phenomena in fluid flows. CFD-based models demonstrate high versatility and capability of dealing with a wide range of engineering problems. This article presents two examples of CFD-based computational modeling successfully applied for different fields of engineering: particle engineering by drying processes and thermal management of car compartment.

**Index Terms**—car thermal management, computational fluid dynamics, particle engineering, transport phenomena

## I. INTRODUCTION

MANY contemporary engineering problems involve flows of liquid and/or gas, transport of heat by conduction, convection and radiation mechanisms, mass transfer by diffusion and convection, flows of bubbles, drops or particles, combustion etc. These complex problems require fundamental understanding that cannot be provided only by available experimental techniques, and therefore theoretical and numerical modeling are essential.

Recent progress in computer industry stimulated fast development of computational approaches and numerical methods, among them Computational Fluid Dynamics (CFD). This is a wide spread modeling approach which utilizes numerical methods and computer simulations to solve and analyze problems that involve transport phenomena in fluid flows. Lots of commercial and open computer codes are implementing CFD technique: ANSYS FLUENT, ANSYS CFX, FLOW-3D, STAR-CD, COMSOL CFD, OpenFOAM, OpenFVM and many others.

This contribution presents two examples of CFD-based computational modeling successfully applied for different fields of engineering: particle engineering by drying processes and thermal management of car compartment. In spite of apparent differences, these two models have common roots in description of transport phenomena of the gas phase that presented in the both considered cases.

## II. PARTICLE ENGINEERING BY DRYING PROCESSES

### A. Spray Drying

Spray drying is a widely applied technology used to transform solutions, emulsions or suspensions into dry granules, particle agglomerates or powder, by feeding the liquid mixture as a spray of droplets into a medium with a hot drying agent. Because spray drying can be used either as a preservation method or simply as a fast drying technique, this process is utilized in many industries, such as food manufactures, pharmaceutical, chemical and biochemical industries. Spray drying is a rapid process (up to several seconds) compared to other methods of drying (e.g., pulse combustion drying, drum drying, freeze drying) due to the small spray droplet sizes and their large specific surface areas that maximize rates of heat and mass transfer. Therefore, this technique is the preferred drying method for many thermally-sensitive materials. Spray drying also turns a raw material into a dried powder in a single step, which can be advantageous for profit maximization and process simplification. Along with other drying techniques, spray drying also provides the advantage of weight and volume reduction. Dyestuffs, paint pigments, plastics, resins, catalysts, ceramic materials, washing powders, pesticides, fertilizers, organic and inorganic chemicals, skim and whole milk, baby foods, instant coffee and tea, dried fruits, juices, eggs, spices, cereal, enzymes, vitamins, flavors, antibiotics, medical ingredients, additives, animal feeds, biomass – this list of the spray-dried products is far from being complete.

A typical spray drying tower includes an atomizer, which transforms the supplied liquid feed into a spray of droplets, and a contact mixing zone, where the spray interacts with a hot drying agent. As a result of this interaction, the moisture content of the drying agent increases due to liquid evaporation from the droplets. In turn, due to evaporation, the spray droplets shrink and turn into solid particles. The drying process proceeds until the dried particles with the desired moisture content are obtained and then the final product is recovered from the drying chamber. Depending on the process needs, droplet sizes from 1 to 1000  $\mu\text{m}$  can be achieved; for the most common applications average spray droplet diameters are between 100 to 200  $\mu\text{m}$ . Air under atmospheric pressure, steam and inert gases like nitrogen are popular drying agents used nowadays. It is noted that inert gases are applied for drying flammable, toxic or oxide-sensitive materials.

### B. Pneumatic Drying

Pneumatic (flash) drying is another example of extensively used technology in food, chemical, agricultural

Manuscript received March 6, 2012; revised April 10, 2012.

M. Mezhericher is with the Mechanical Engineering Department, Sami Shamoon College of Engineering, Israel (phone: 972-8-647-5075; fax: 972-8-647-5749; e-mail: maksime@sce.ac.il).

and pharmaceutical industries. The main advantages of this process are fast elimination of free moisture from pre-prepared feed of wet particles and operation in continuous mode. Typically, the feed is introduced into the drying column by a screw via a Venturi pipe. The particles dry out in seconds as they are conveyed by hot gas (air) stream. Then, the product is separated using cyclones which are usually followed by scrubbers or bag filters for final cleaning of the exhaust gases. In spite of its apparent simplicity, the process of pneumatic drying is a complex multi-scale multi-phase transport phenomenon involving turbulent mixing of humid gas and multi-component wet particles, heat and mass transfer interaction between the drying gas and dispersed phase, and internal heat and moisture transport within each conveyed wet particle.

### III. THERMAL MANAGEMENT OF CAR COMPARTMENT

One of the most energy-expensive units in contemporary vehicles is the air conditioning system (ACS). On an average, such systems consume up to 17% of the overall power produced by vehicle engines of the world, depending on the cooling regime and environment thermal load [1]. It is remarkable that air-conditioning units in cars and light commercial vehicles burn more than 5% of the vehicle fuel consumed annually throughout the European Union [2]. For instance, the United Kingdom emits about 3 million tones of CO<sub>2</sub> each year simply from powering the air-conditioning systems in vehicles. In South European and Mediterranean countries the problem of air pollution increase by ACS powering is even more acute.

Extensive theoretical and experimental studies have been performed throughout the recent years, aimed to reduce the fuel consumption and environmental pollution due to vehicle air conditioning. Proper thermal management based on the gas dynamics inside the vehicle passenger compartment is crucial for air conditioning and heating systems performance as well as for the comfort of the passengers. On the other hand, the nature of the flow, namely the velocity field in combination with the temperature distribution, has a strong influence on the human sensation of thermal comfort [3].

In the present research it is proposed to develop a three-dimensional theoretical model of transport phenomena in car compartment. This model is based on Eulerian approach for the gas flow and takes into account thermal energy transfer by simultaneous conduction, convection and radiation mechanisms within the compartment as well as outside the vehicle. The model is able to predict steady-state and transient profiles of air velocity, density, pressure, temperature and humidity for various regimes of the air conditioning, vehicle driving modes, compartment configurations and ambient conditions.

To assess the passenger level of thermal comfort, a methodology based on published studies [4,5] might be developed and the corresponding equations might be coupled to the developed computational model. Moreover, the effect of the passengers themselves on their thermal comfort (e.g., heat emission by human body, air inhalation and gas mixture exhalation etc.) might be considered.

The CFD-based model of thermal management can be utilized as a tool for the following parametric investigations: enhancement of natural convection within a compartment,

influence of thermal insulation and trim materials on the passenger thermal comfort as well as effect of introduction of innovating passive cooling techniques on energy consumption by ACS.

## IV. THEORETICAL MODELING

### A. Spray and Pneumatic Drying

Transport phenomena in drying processes is subdivided into *external* (gas-particles mixing) and *internal* (within dispersed droplets/particles).

The fluid dynamics of continuous phase of drying gas is treated by an Eulerian approach and a standard k-ε model is utilized for turbulence description. The utilized three-dimensional conservation equations of continuity, momentum, energy, species, turbulent kinetic energy and dissipation rate of turbulence kinetic energy are as follows (i, j = 1, 2, 3):

- continuity

$$\frac{\partial \rho}{\partial t} + \frac{\partial}{\partial x_j} (\rho u_j) = S_c, \quad (1)$$

where  $\rho$  and  $u$  are drying gas density and velocity, and  $S_c$  is mass source term.

- momentum conservation

$$\frac{\partial}{\partial t} (\rho u_i) + \frac{\partial}{\partial x_j} (\rho u_i u_j) = - \frac{\partial p}{\partial x_i} + \frac{\partial}{\partial x_j} \left[ \mu_e \left( \frac{\partial u_i}{\partial x_j} + \frac{\partial u_j}{\partial x_i} \right) \right] + \Delta \rho g_i + U_{pi} S_c + \sum F_{sp}, \quad (2)$$

where  $p$  and  $\mu_e$  are drying gas pressure and effective viscosity,  $U_p$  is particle velocity and  $\sum F_{sp}$  is sum of the forces exerted by particles on the gas phase.

- energy conservation

$$\frac{\partial}{\partial t} (\rho h) + \frac{\partial}{\partial x_j} (\rho u_j h) = \frac{\partial}{\partial x_j} \left( \frac{\mu_e}{\sigma_h} \frac{\partial h}{\partial x_j} \right) - q_r + S_h, \quad (3)$$

where  $h$  is specific enthalpy,  $q_r$  and  $S_h$  are thermal radiation and energy source terms, respectively.

- species conservation

$$\frac{\partial}{\partial t} (\rho Y_v) + \frac{\partial}{\partial x_j} (\rho u_j Y_v) = \frac{\partial}{\partial x_j} \left( \frac{\mu_e}{\sigma_Y} \frac{\partial Y_v}{\partial x_j} \right) + S_c, \quad (4)$$

where  $Y_v$  is mass fraction of vapour in humid gas.

- turbulence kinetic energy

$$\frac{\partial}{\partial t} (\rho k) + \frac{\partial}{\partial x_j} (\rho u_j k) = \frac{\partial}{\partial x_j} \left( \frac{\mu_e}{\sigma_k} \frac{\partial k}{\partial x_j} \right) + G_k + G_b - \rho \varepsilon, \quad (5)$$

where  $k$  is turbulent kinetic energy and  $\varepsilon$  is dissipation rate of turbulent kinetic energy.

- dissipation rate of turbulence kinetic energy

$$\frac{\partial}{\partial t} (\rho \varepsilon) + \frac{\partial}{\partial x_j} (\rho u_j \varepsilon) = \frac{\partial}{\partial x_j} \left( \frac{\mu_e}{\sigma_\varepsilon} \frac{\partial \varepsilon}{\partial x_j} \right) + \frac{\varepsilon}{k} (C_1 G_k - C_2 \rho \varepsilon). \quad (6)$$

The production of turbulence kinetic energy due to mean velocity gradients is equal to:

$$G_k = \mu_T \left( \frac{\partial u_i}{\partial x_j} + \frac{\partial u_j}{\partial x_i} \right) \frac{\partial u_i}{\partial x_j}. \quad (7)$$

The production of turbulence kinetic energy due to buoyancy is given by:

$$G_b = -\beta g_j \frac{\mu_T}{\sigma_T} \frac{\partial T}{\partial x_j}, \quad (8)$$

where  $T$  is gas temperature and  $\beta$  is coefficient of gas thermal expansion:

$$\beta = -\frac{1}{\rho} \left( \frac{\partial \rho}{\partial T} \right)_p. \quad (9)$$

The utilized constants are  $C_1 = 1.44$ ,  $C_2 = 1.92$ , and the Prandtl numbers are equal to  $\sigma_k = \sigma_h = \sigma_y = \sigma_T = 0.9$  and  $\sigma_\epsilon = 1.3$ . The effective viscosity,  $\mu_e$ , is defined as:

$$\mu_e = \mu + \mu_T, \quad (10)$$

where  $\mu_T$  is turbulent viscosity

$$\mu_T = C_\mu \rho \frac{k^2}{\epsilon}. \quad (11)$$

In the above expression  $C_\mu = 0.09$ .

The constitutive relationship between air temperature, pressure and density is given by the ideal gas law (such model is sufficient because of small humidity of the gas involved in the considered multiphase flow):

$$p = \frac{\rho}{M} \mathfrak{R} T, \quad (12)$$

where  $\mathfrak{R}$  is universal gas constant and  $M$  is molecular weight of the gas phase.

To track the trajectories and other valuable parameters of spray of droplets and particles, a Discrete Phase Model (DPM) based on Lagrangian formulation is utilized. The motion of the droplets/particles is described by Newton's Second Law:

$$\frac{d\vec{U}_p}{dt} = \vec{g} + \frac{\sum \vec{F}_p}{m_p}. \quad (13)$$

Here  $\sum \vec{F}_p$  is sum of the forces exerted on given spray droplet/particle by the gas phase, by other particles and walls of the spray drying chamber;  $\vec{g}$  is gravity acceleration, and  $\vec{U}_p$  and  $m_p$  are droplet/particle velocity and mass, respectively. In general, the acting forces on spray droplet/particle are as follows:

$$\sum \vec{F}_p = \vec{F}_D + \vec{F}_B + \vec{F}_A + \vec{F}_{PG} + \vec{F}_C + \vec{F}_{other}, \quad (14)$$

where  $\vec{F}_D$  is drag force,  $\vec{F}_B$  is buoyancy force,  $\vec{F}_A$  is added mass force,  $\vec{F}_{PG}$  is pressure gradient force and  $\vec{F}_C$  is contact force. The term  $\vec{F}_{other}$  represents other forces, usually important for submicron particles and/or at specific conditions, e.g., phoretic, Basset, Saffman, Magnus forces etc., and neglected in the present work for simplicity.

The drag force is determined by the expression:

$$\vec{F}_D = \frac{\pi d_p^2}{8} \rho C_D |\vec{u} - \vec{U}_p| (\vec{u} - \vec{U}_p), \quad (15)$$

where  $d_p$  is droplet/particle diameter and  $\vec{u}$  is velocity of gas phase. The drag coefficient,  $C_D$ , is calculated according to well-known empirical correlations for spherical particles.

The buoyancy force opposes gravity and in the present study it is much smaller than the latter, because the densities of spray droplets and drying gas differ more than thousand times. For this reason the buoyancy of droplets/particles is currently neglected.

The added mass ("virtual-mass") force, required to accelerate the gas surrounding the droplet/particle, is given by:

$$\vec{F}_A = \rho \frac{\pi d_p^3}{12} \frac{d}{dt} (\vec{u} - \vec{U}_p). \quad (16)$$

For flow in dryers, this force may be important in the droplets/particles entrance region, where the velocities of injected dispersed phase and drying gas are substantially different and their intensive mixing leads to high change rates of the relative velocities.

The pressure gradient in the gas phase additionally accelerates droplets/particles and results in the following force:

$$\vec{F}_{GP} = -\frac{\pi d_p^3}{6} \vec{\nabla} p. \quad (17)$$

This force can be essential and worth consideration in the dryer regions with fast pressure changes like inlet, outlet and swirling zones of the gas phase.

The contact force arises from collision interactions between the given droplet/particle with other droplets/particles or walls of the drying chamber. At the current step these interactions are not considered and correspondingly the contact force is neglected, because the focus of this work was on implementation of previously developed description of internal transport phenomena in the dispersed phase.

In the present work the *internal transport phenomena* within each droplet/particle are described with the help of previously developed and validated two-stage drying kinetics model, see [6]. The drying process of droplet containing solids is divided in two drying stages. In the first stage of drying, an excess of moisture forms a liquid envelope around the droplet solid fraction, and unhindered drying similar to pure liquid droplet evaporation results in the shrinkage of the droplet diameter. At a certain moment, the moisture excess is completely evaporated, droplet turns into a wet particle and the second stage of a hindered drying begins. In this second drying stage, two regions of wet particle can be identified: layer of dry porous crust and internal wet core. The drying rate is controlled by the rate of moisture diffusion from the particle wet core through the crust pores towards the particle outer surface. As a result of the hindered drying, the particle wet core shrinks and the thickness of the crust region increases. The particle outer diameter is assumed to remain unchanged during the second drying stage. After the point when the particle moisture content decreases to a minimal possible value (determined either as an equilibrium moisture content or as a bounded moisture that cannot be removed by drying), the particle is treated as a dry non-evaporating solid sphere. It is worth noting that all droplets and particles are assumed to be spherical and a full radial symmetry of inter-droplet physical

parameters (temperature, moisture content etc.) is believed. The concept of two-stage droplet drying kinetics is illustrated by Fig. 1.

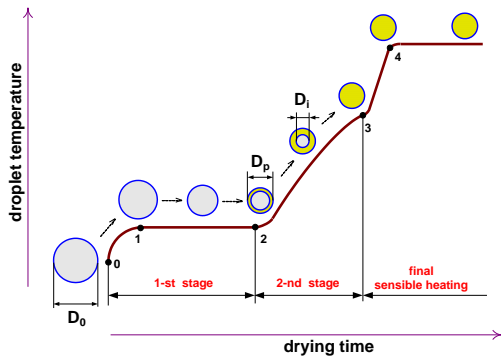


Fig. 1. Concept of two-stage droplet drying kinetics [6].

### B. Thermal Management of Car Compartment

The conservation equations of the above 3D model of transport phenomena in particle engineering processes can also be applied to describe the gas flow and heat and mass transfer within a car passenger compartment and in its surroundings. Particularly, in the present study 3D compressible Reynolds Averaged Navier-Stokes (RANS) equations including  $k-\epsilon$  turbulence formulation (1)-(12) are utilized to predict flow patterns of the gas mixture (air, vapor, CO<sub>2</sub>) inside a passenger compartment and air flow outside the cabin. These equations are solved by applying a Finite Volumes Method (FVM). The computational model formulated in such way is capable of predicting air velocity, temperature and species flow patterns inside the compartment under different ambient conditions. Moreover, the model can be used to prognosticate energy consumption of ACS that is necessary for providing passengers comfort at given outside thermal load. In addition, numerical simulations with this 3D model may facilitate revealing weak points and optimization of existing/newly designed car air conditioning systems.

## V. NUMERICAL SIMULATIONS

### A. Spray Drying

A cylinder-on-cone spray dryer with co-current flow of drying air and spray of droplets (Fig. 2) is adopted from the literature [6]. A centrifugal pressure nozzle atomizer is located at the top of the drying chamber and the drying air enters the top of the chamber through an annulus without swirling at angle of 35° with respect to the vertical axis.

Preheated atmospheric air at temperature 468 K and absolute humidity of 0.009 kg H<sub>2</sub>O/kg dry air is supplied into the drying chamber through a central round inlet of the flat horizontal ceiling. The air inlet velocity is 9.08 m/s, whereas its turbulence kinetic energy is equal to 0.027 m<sup>2</sup>/s<sup>2</sup> and turbulence energy dissipation rate is 0.37 m<sup>2</sup>/s<sup>3</sup>. The spray of liquid droplets is obtained by atomizing the liquid feed in the nozzle. The spray cone angle is assumed to be 76°, the droplet velocities at the nozzle exit are assigned to 59 m/s, and the temperature of the feed is set at 300 K. The distribution of droplet diameters in the spray is assumed to obey the Rosin-Rammler distribution function, where the

mean droplet diameter is assumed to be 70.5 μm, the spread parameter is set at 2.09, and the corresponding minimum and maximum droplet diameters are taken as 10.0 μm and 138.0 μm, respectively. The overall spray mass flow rate is equal to 0.0139 kg/s (50 kg/hr). The walls of drying chamber are assumed to be made of 2-mm stainless steel, and the coefficient of heat transfer through the walls is set to zero as though there is a perfect thermal insulation of the chamber. Finally, the gage air pressure in the outlet pipe of the drying chamber is set to -100 Pa.

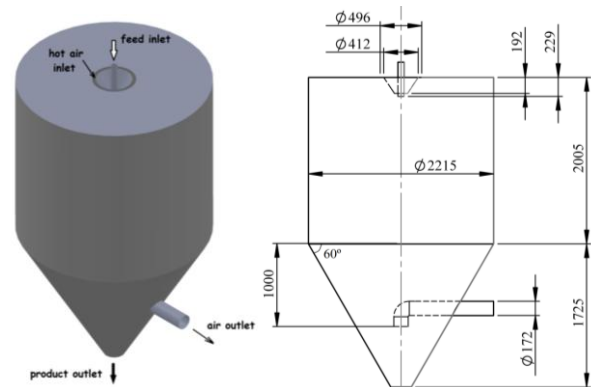


Fig. 2. Spray dryer setup used in the study. Left picture - isometric view, right picture - sketch of the adopted chamber geometry.

The numerical solution of the model equations and computational simulations have been performed by utilizing a 3D pressure-based solver incorporated in CFD package ANSYS FLUENT 13. The solver is based on the finite volumes technique and enables two-way coupled Euler-DPM algorithm for treatment of the continuous and discrete phases. The chamber geometry has been meshed by 619,711 unstructured grid cells of tetrahedral and polyhedral shape with the various mesh sizes. Particularly smaller mesh volumes are located in the regions of high concentration of the discrete phase in the downstream direction of the spray injection, where large gradients of momentum, heat and mass transfer are expected to occur. Correspondingly, grid cells of the larger sizes are located near the top and side walls of the chamber.

The 3D spray from pressure nozzle is modeled by 20 spatial droplet streams. In turn, each droplet stream is represented by 10 injections of different droplet diameters: minimum and maximum diameters are 10.0 μm and 138.0 μm, whereas the intermediate droplet sizes are calculated by applying Rosin-Rammler distribution function with 70.5 μm of droplet average size. In this way, totally 200 different droplet injections have been introduced into the computational domain.

All the numerical simulations of spray drying process have been performed in steady-state two-way coupling mode of calculations. For continuous phase, the spatial discretization was performed by upwind scheme of second order for all conservation equations (except pressure solved by PRESTO! procedure) and SIMPLE scheme was used for coupling between the pressure and velocity. For the dispersed phase, the tracking scheme was automatically selected between low order implicit and high order trapezoidal schemes based on the solution stability. DPM sources were updated every iteration of the continuous

phase. The overall steady-state numerical formulation was of the second order of accuracy.

The computation of internal transport phenomena for the discrete phase was accomplished using the concept of user defined functions (UDF). In this way, the first drying stage and the final heating of non-evaporating dry particles were simulated using the ANSYS FLUENT built-in functions responsible for evaporation and sensible heating of droplets. For the second drying stage, the set of corresponding equations was solved for each wet particle using the original numerical algorithm described in details by Mezhericher [6]. This numerical solution was implemented as a subroutine and linked to the ANSYS FLUENT solver via a set of the original UDFs. The decision whether the built-in functions or the UDFs of the second drying stage should be used for the specific spray particle at the given calculation step was made automatically by the solver based on the current particle moisture content.

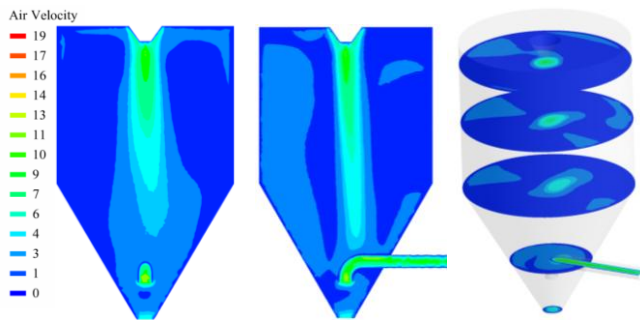


Fig. 3. Flow fields of air velocity (m/s): frontal (left), side (middle) and isometric (right) cuts.



Fig. 4. Flow patterns of air temperature (Kelvin): frontal (left), side (middle) and isometric (right) cuts.

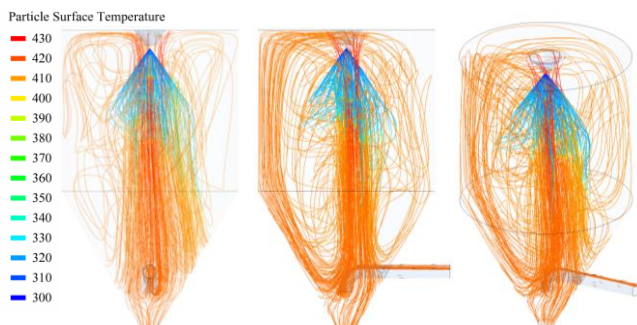


Fig. 5. Particle trajectories colored by particle surface temperature (Kelvin): frontal (left), side (middle) and isometric (right) views.

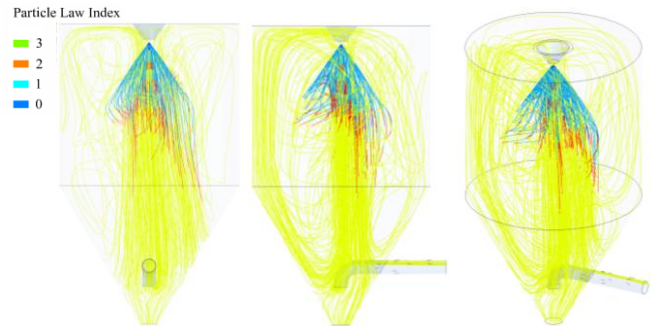


Fig. 6. Particle trajectories colored by particle law index: frontal (left), side (middle) and isometric (right) views. Here “0” means droplet initial heating, “1” corresponds to droplet evaporation, “2” indicates second drying stage (wet particle drying) and “3” designates particle final sensible heating.

### B. Pneumatic Drying

For the purposes of the theoretical study the geometry of Baeyens et al. [7] experimental set-up is adopted. Hot dry air and wet particles are supplied to the bottom of vertical pneumatic dryer with 1.25 m internal diameter and 25 m height (see Fig. 1).

The developed theoretical model was numerically solved with the help of Finite Volume Method and 3D simulations of pneumatic drying were performed using the CFD package FLUENT. For these purposes, the 3D numerical grid with 9078 distributed hexahedral/wedge cell volumes was generated in GAMBIT 2.2.30 using the Cooper scheme.

The flow of wet particles in the pneumatic dryer was simulated through 89 injections of spherical particles. Each injection began on the bottom of the dryer at the centroid of one of the 89 bottom plane mesh elements. The particle injections were normal to the dryer bottom plane and parallel to each other.

The numerical simulations were performed in the following way. First, the flow of drying air was simulated without the discrete phase until converged solution. At the next step, wet particles were injected into the domain and two-way coupled simulations were performed until convergence.

The convergence of the numerical simulations was monitored by means of residuals of the transport equations. Particularly, the converged values of the scaled residuals were ensured to be lower than  $10^{-6}$  for the energy equation and  $10^{-3}$  for the rest of equations. The convergence was also verified by negligibly small values of the global mass and energy imbalances.

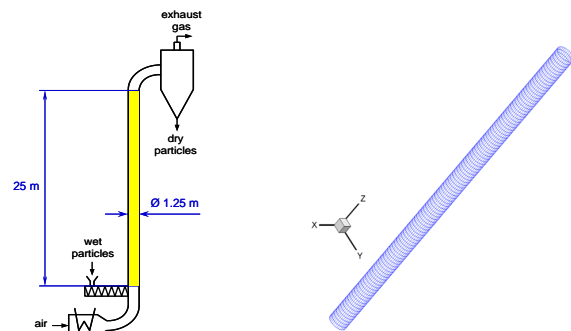


Fig. 7. Schematic sketch of pneumatic dryer setup [7] (left) and utilized numerical grid (right).

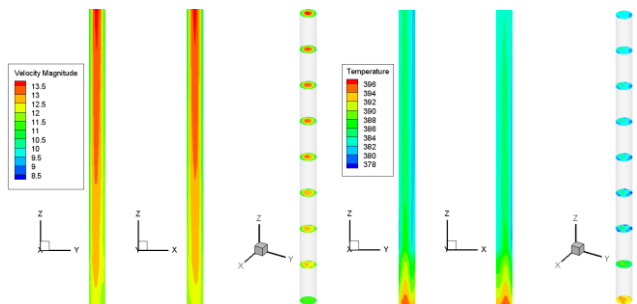


Fig. 8. 3D air flow patterns for PVC drying in pneumatic dryer (adiabatic flow). Left – velocity magnitude, m/s, right – temperature, K.

### C. Air Flow Patterns in Car Passenger Compartment

A simplified model of conventional car passenger compartment was adopted for numerical simulations. The original car model was created in 3D Studio Max software whereas the extracted compartment geometry was processed in ANSYS ICEM CFD program and meshed with 518,705 polyhedral (3-6 faces) grid cells. Then, steady state 3D numerical simulations using ANSYS FLUENT code were performed.



Fig. 9. Car model in 3D Studio Max software (left) and extracted compartment geometry (right).

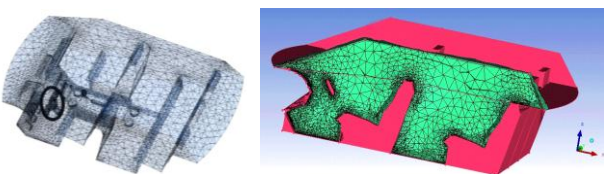


Fig. 10. Numerical grid used in the flow simulations

Figures 11-13 demonstrates the results of numerical simulations of air flow patterns in the compartment. Four air inlets with velocity 1 m/s and temperature 12 °C and two air outlets with -150 Pa gage pressure were assumed. The ambient temperature was taken 37 °C and heat transfer coefficient was set to 10 W/(m<sup>2</sup>·K), assuming parked car.

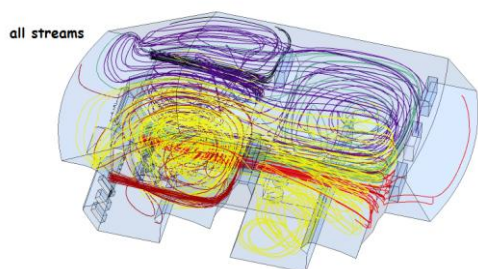


Fig. 11. Simulated streamlines of steady-state air velocity in car compartment.

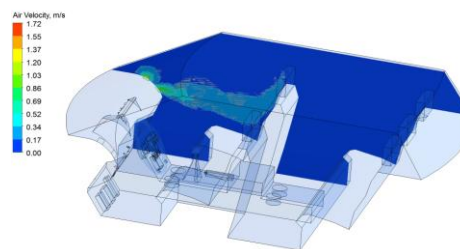


Fig. 12. Simulated contours of air velocity in car compartment (m/s, representative vertical cut).

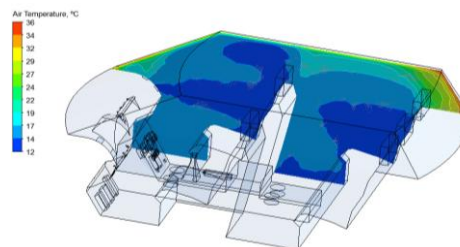


Fig. 13. Simulated contours of air temperature in car compartment (°C, representative vertical cut).

## VI. CONCLUSION

- Computational CFD-based modelling is a powerful tool for description, simulation and analysis of variety of engineering problems involving macroscopic transport phenomena (fluid/gas dynamics, turbulence, heat transfer and mass transfer).
- CFD-based models demonstrate high versatility and capability of dealing with a wide range of engineering problems.
- Numerical simulations utilizing CFD-based models can substantially reduce amount of necessary experiments, time and overall cost of solution of many engineering and scientific problems.
- Basic knowledge in CFD-based modelling and ability to work with CFD software are becoming to be necessary skills for contemporary engineers and researchers.

## REFERENCES

- [1] M.A. Lambert, and B.J. Jones, "Automotive Adsorption Air Conditioner Powered by Exhaust Heat. Part 1: Conceptual and Embodiment Design", *J. Automobile Engineering*, vol. 220, no. 7, pp. 959-972, 2006.
- [2] *Sorption Energy Seeking to Commercialize Waste Heat-Driven Adsorption Heat Pump Technology for Vehicle Air Conditioning*. Green Car Congress <http://www.greencarcongress.com>, 24 April 2010.
- [3] *Application Briefs from FLUENT. EX170. Vehicle Ventilation System*. [http://www.fluent.com/solutions/automotive/ex170\\_vehicle\\_ventilation\\_system.pdf](http://www.fluent.com/solutions/automotive/ex170_vehicle_ventilation_system.pdf)
- [4] L. Huang and T.A. Han, "Case Study of Occupant Thermal Comfort in a Cabin Using Virtual Thermal Comfort Engineering", in *Proc. EACC 2005 - 2nd European Automotive CFD Conference*, Frankfurt, Germany, 29 - 30 June 2005.
- [5] G. Lombardi, M. Maganzi, F. Cannizzo and G. Solinas, "The Use of CFD to Improve the Thermal Comfort in the Automotive Field", in *Proc. EACC 2007 - 3rd European Automotive CFD Conference*, Frankfurt, Germany, 5 - 6 July 2007.
- [6] M. Mezhericher, *Theoretical modeling of spray drying processes. Volume 1. Drying kinetics, two and three dimensional CFD modeling*. LAP Lambert Academic Publishing, Saarbrücken, Germany, 2011. ISBN 978-3-8443-9959-2.
- [7] J. Baeyens, D. van Gauwbergen and I. Vinckier, "Pneumatic drying: the use of large-scale experimental data in a design procedure", *Powder Technology*, vol. 83, pp. 139-148, 1995.